



HAL
open science

Rogue waves in shallow water in the presence of a vertically sheared current

Christian Kharif, Malek Abid, Julien Touboul

► **To cite this version:**

Christian Kharif, Malek Abid, Julien Touboul. Rogue waves in shallow water in the presence of a vertically sheared current. *Journal of Ocean Engineering and Marine Energy*, 2017, 3 (4), pp.301 - 308. 10.1007/s40722-017-0085-7. hal-01785636

HAL Id: hal-01785636

<https://hal.science/hal-01785636>

Submitted on 4 May 2018

HAL is a multi-disciplinary open access archive for the deposit and dissemination of scientific research documents, whether they are published or not. The documents may come from teaching and research institutions in France or abroad, or from public or private research centers.

L'archive ouverte pluridisciplinaire **HAL**, est destinée au dépôt et à la diffusion de documents scientifiques de niveau recherche, publiés ou non, émanant des établissements d'enseignement et de recherche français ou étrangers, des laboratoires publics ou privés.

1 **Rogue waves in shallow water in the presence of a**
2 **vertically sheared current**

3 **Christian Kharif · Malek Abid · Julien**
4 **Touboul**

5
6 Received: date / Accepted: date

7 **Abstract** Two-dimensional rogue wave occurrence in shallow water on a ver-
8 tically sheared current of constant vorticity is considered. Using Euler equa-
9 tions and Riemann invariants in the shallow water approximation, hyperbolic
10 equations for the surface elevation and the horizontal velocity are derived and
11 closed-form nonlinear evolution equation for the surface elevation is obtained.
12 Following Whitham (1974), a dispersive term is added to this equation us-
13 ing the fully linear dispersion relation. With this new single first-order partial

C. Kharif

Aix Marseille Université, CNRS, Centrale Marseille, IRPHE UMR 7342, F-13384, Marseille,
France

E-mail: kharif@irphe.univ-mrs.fr

M. Abid

Aix Marseille Université, CNRS, Centrale Marseille, IRPHE UMR 7342, F-13384, Marseille,
France

J. Touboul

Université de Toulon, Aix Marseille Université, CNRS, IRD, Mediterranean Institute of
Oceanography (MIO), La Garde, France

Aix Marseille Université, Université de Toulon, CNRS, IRD, Mediterranean Institute of
Oceanography (MIO), Marseille, France

14 differential equation, vorticity effects on rogue wave properties are studied nu-
15 merically. Besides, the Boundary Integral Element Method (BIEM) and the
16 KdV equation both with vorticity are used for this numerical investigation,
17 too. It is shown that results from the generalised Whitham equation agree quite
18 well with those from BIEM whereas those from the KdV model are quite dif-
19 ferent. The numerical simulations carried out with the generalised Whitham
20 equation and BIEM show that the presence of an underlying vertically sheared
21 current modifies rogue wave properties significantly. For negative vorticity the
22 amplification factor and duration of extreme wave events are increased whereas
23 it is the opposite for positive vorticity.

24 **1 Introduction**

25 Generally, in coastal and ocean waters, current velocity profiles are established
26 by bottom friction and wind stress at the sea surface, and consequently are
27 vertically varying. Ebb and flood currents due to the tide may have an impor-
28 tant effect on water wave properties. In any region where the wind blows, the
29 generated current affects the behavior of the waves. The present work focuses
30 on the nonlinear evolution of two-dimensional gravity waves propagating in
31 shallow water on a shear current which varies linearly with depth. We assume
32 that the directional spread of the wave field is sufficiently narrow to consider
33 unidirectional propagation of the waves.

34 There are a number of physical mechanisms that focus the wave energy into a
35 small area and produce the occurrence of extreme waves called freak or rogue
36 waves. These events may be due to refraction (presence of variable currents or
37 bottom topography), dispersion (frequency modulation), wave instability (the
38 modulational instability), soliton interactions, crossing seas, etc. For more de-
39 tails on these different mechanisms see the reviews on freak waves by Kharif
40 and Pelinovsky (2003), Dysthe et al (2008), Kharif et al (2009) and Onorato
41 et al (2013). Few studies have been devoted to the occurrence of extreme wave
42 events in shallow water. Among the authors who have investigated rogue wave

43 properties in shallow water, one can cite Pelinovsky et al (2000) , Kharif et al
44 (2000), Peterson et al (2003), Soomere and Engelbrecht (2005), Talipova et al
45 (2008) and Chambarel et al (2010). Pelinovsky and Sergeeva (2006) and Toffoli
46 et al (2006) investigated the statistical properties of rogue waves in shallow
47 water.

48 To the best of our knowledge, there is no paper on the effect of a vertically
49 sheared current on rogue wave properties apart from that of Touboul and
50 Kharif (2016) in deep water. We propose to extend this work to the case of
51 shallow water.

52 Within the framework of the shallow water wave theory Whitham (1974) pro-
53 posed a generalised equation governing the evolution of fully nonlinear waves
54 satisfying the full linear dispersion. The Whitham equation may be derived
55 from the previous generalised Whitham equation assuming that the waves
56 are weakly nonlinear. The Whitham equation and the KdV equation which
57 have the same nonlinear term differ from each other by the dispersive term.
58 Very recently, Hur and Johnson (2015) have considered a modified Whitham
59 equation taking account of constant vorticity. Very recently, Kharif and Abid
60 (2017) have proposed a new model derived from the Euler equations for wa-
61 ter waves propagating on a vertically sheared current of constant vorticity in
62 shallow water. The heuristic introduction of dispersion allows the study of
63 strongly nonlinear two-dimensional long gravity waves in the presence of vor-
64 ticity. Consequently, this new equation extends to waves propagating in the
65 presence of vorticity the generalised Whitham equation.

66 Two different approaches are used to investigate rogue waves propagating
67 in shallow water on a shear current of constant vorticity: the generalised
68 Whitham equation with vorticity and the Boundary Integral Element Method
69 (BIEM) which allows the study of fully nonlinear dispersive water waves on
70 arbitrary depth in the presence of vorticity (see Touboul and Kharif (2016)).
71 Besides, a numerical investigation is carried out by using the KdV equation
72 with constant vorticity whose derivation can be found in the papers by Free-

73 man and Johnson (1970) and Choi (2003). Note that the latter equation can
 74 be derived from the generalised Whitham equation with vorticity assuming
 75 that the waves are weakly nonlinear and weakly dispersive.

76 **2 Two mathematical formulations**

77 2.1 The generalised Whitham equation with vorticity

78 We consider two-dimensional gravity water waves propagating at the free sur-
 79 face of a vertically sheared current of uniform intensity Ω which is the opposite
 80 of the vorticity. The wave train moves along the x – axis and the z – axis is
 81 oriented upward opposite to the gravity. The origin $z = 0$ is the undisturbed
 82 free surface and $z = -h$ is the rigid horizontal bottom.

83 The continuity equation is

$$u_x + w_z = 0 \quad (1)$$

84 where u and w are the longitudinal and vertical components of the *wave in-*
 85 *duced velocity*, respectively. The underlying current is $U = U_0 + \Omega z$ where U_0
 86 is the constant surface velocity.

87 Integrating equation (1) and using the boundary conditions at the free surface
 88 and at the bottom we obtain the following equation

$$\eta_t + \frac{\partial}{\partial x} [u(\eta + h) + \frac{\Omega}{2}\eta^2 + U_0\eta] = 0 \quad (2)$$

89 where u is assumed to be independent of z .

90 Equation (2) corresponds to mass conservation in shallow water in the pres-
 91 ence of constant vorticity.

92 Under the assumption of hydrostatic pressure, the Euler equation in x -direction
 93 is

$$u_t + (u + U_0 + \Omega z)u_x + \Omega w + g\eta_x = 0 \quad (3)$$

94 where g is the gravity.

95 Using the continuity equation and boundary conditions that w satisfies on the
 96 bottom and at the free surface, we obtain

$$w = -(z + h)u_x \quad (4)$$

97 It follows that the Euler equation becomes

$$u_t + (u + U_0 - \Omega h)u_x + g\eta_x = 0 \quad (5)$$

98 The dynamics of non dispersive shallow water waves on a vertically sheared
 99 current of constant vorticity is governed by equations (2) and (5) that admit a
 100 pair of Riemann invariants. These Riemann invariants which are derived ana-
 101 lytically allows us to express the longitudinal component of the wave induced
 102 velocity $u(x, t)$ as a function of the elevation η . Finally, equations (2) and (5)
 103 can be reduced to the following single nonlinear partial differential equation
 104 for η

$$\eta_t + \left\{ U_0 - \frac{\Omega h}{2} + 2\sqrt{g(\eta + h) + \Omega^2(\eta + h)^2/4} - \sqrt{gh + \Omega^2 h^2/4} \quad + \right. \\ \left. \frac{g}{\Omega} \ln \left[1 + \frac{\Omega}{2g} \frac{\Omega\eta + 2(\sqrt{g(\eta + h) + \Omega^2(\eta + h)^2/4} - \sqrt{gh + \Omega^2 h^2/4})}{1 + \frac{\Omega}{g}(\frac{\Omega h}{2} + \sqrt{gh + \Omega^2 h^2/4})} \right] \right\} \eta_x = 0 \quad (6)$$

105 This equation is fully nonlinear and describes the spatio-temporal evolution of
 106 hyperbolic water waves propagating rightwards in shallow water in the pres-
 107 ence of constant vorticity.

108 Following Whitham (1974), full linear dispersion is introduced heuristically

$$\eta_t + \left\{ U_0 - \frac{\Omega h}{2} + 2\sqrt{g(\eta + h) + \Omega^2(\eta + h)^2/4} - \sqrt{gh + \Omega^2 h^2/4} \quad + \right. \\ \left. \frac{g}{\Omega} \ln \left[1 + \frac{\Omega}{2g} \frac{\Omega\eta + 2(\sqrt{g(\eta + h) + \Omega^2(\eta + h)^2/4} - \sqrt{gh + \Omega^2 h^2/4})}{1 + \frac{\Omega}{g}(\frac{\Omega h}{2} + \sqrt{gh + \Omega^2 h^2/4})} \right] \right\} \eta_x + K * \eta_x = 0 \quad (7)$$

109 where $K * \eta_x$ is a convolution product. The kernel K is given as the inverse
 110 Fourier transform of the fully linear dispersion relation of gravity waves in

111 finite depth in the presence of constant vorticity Ω : $K = F^{-1}(c)$ with

$$c = \sqrt{gh} \left(\sqrt{\frac{\tanh(kh)}{kh} \left(\frac{\Omega^2 \tanh(kh)}{4gk} + 1 \right)} - \frac{\Omega \tanh(kh)}{2k\sqrt{gh}} \right)$$

112 Equation (7) governs the propagation of nonlinear long gravity waves in a fully
113 linear dispersive medium. For $\Omega = 0$ and $U_0 = 0$, (6) reduces to generalised
114 equation (13.97) of Whitham (1974).

115 For weakly nonlinear ($\eta/h \ll 1$) and weakly dispersive ($kh \ll 1$) waves, equa-
116 tion (7) reduces to the KdV equation with vorticity derived by Freeman and
117 Johnson (1970) and Choi (2003) who used multiple scale methods, different to
118 the approach used herein. To set the KdV equation in dimensionless form, h
119 and $\sqrt{h/g}$ are chosen as reference length and reference time which corresponds
120 to $h = 1$ and $g = 1$. The equation reads

$$\eta_t + c_0(\Omega)\eta_x + c_1(\Omega)\eta\eta_x + c_2(\Omega)\eta_{xxx} = 0 \quad (8)$$

121 with

$$c_0 = U_0 - \frac{\Omega}{2} + \sqrt{1 + \Omega^2/4} \quad , \quad c_1 = \frac{3 + \Omega^2}{\sqrt{4 + \Omega^2}} \quad , \quad c_2 = \frac{2 + \Omega^2 - \Omega\sqrt{4 + \Omega^2}}{6\sqrt{4 + \Omega^2}}$$

122

123 The equations (6), (7) and (8) are solved numerically in a periodic domain of
124 length $2L$. The length L is chosen $O(400\delta)$ where δ is a characteristic length
125 scale of the initial condition. The number of grid points is $N_x = 2^{12}$. Spa-
126 tial derivatives are computed in the Fourier space and nonlinear terms in the
127 physical space. The link between the two spaces is made by the Fast Fourier
128 Transform. For the time integration, a splitting technique is used. The equa-
129 tions (6), (7) and (8) could be written as

$$\eta_t + L + N = 0, \quad (9)$$

130 where L and N are linear and nonlinear differential operators in η , respectively.
131 Note that in general the operators L and N do not commute. If the initial
132 condition is η_0 , the exact solution of the previous equation is

$$\eta(t) = e^{-(L+N)t}\eta_0. \quad (10)$$

133 This equation is discretized as follows. Let $t_n = n\Delta t$. We have

$$\eta(t_n) = e^{-(L+N)n\Delta t}\eta_0 = (e^{-L\Delta t/2}e^{-N\Delta t}e^{-L\Delta t/2})^n\eta_0 + O(\Delta t^2), \quad (11)$$

134 and the scheme is globally second order in time. The operator $e^{-L\Delta t/2}$ is
 135 computed exactly in the Fourier space. However, the operator $e^{-N\Delta t}$ is ap-
 136 proximated using a Runge-Kutta scheme of order 4. The time step is chosen
 137 as $\Delta t = 0.005$. Furthermore, the efficiency and accuracy of the numerical
 138 method has been checked against the nonlinear analytical solution of the St-
 139 Venant equations for the dam-break problem in the absence of current and
 140 vorticity ($\Omega = 0$ and $U_0 = 0$). For $U_0 = 0$ and $\Omega = 0$ equation (6) reduces to

$$H_t + (3\sqrt{gH} - 2\sqrt{gh})H_x = 0, \quad \text{with } H = \eta + h. \quad (12)$$

141 For $t > 0$, the nonlinear analytical solution of equation (12) is

$$\begin{aligned} H(x, t) &= h, & u(x, t) &= 0; & \frac{x}{t} &\geq \sqrt{gh} \\ H(x, t) &= \frac{h}{9} \left(2 + \frac{x}{\sqrt{gh}t} \right)^2, & u(x, t) &= -\frac{2}{3} (\sqrt{gh} - \frac{x}{t}); & -2\sqrt{gh} &\leq \frac{x}{t} \leq \sqrt{gh} \\ H(x, t) &= 0, & u(x, t) &= 0; & \frac{x}{t} &\leq -2\sqrt{gh} \end{aligned} \quad (13)$$

142 At time $t = 0$ the initial condition is $H(x, 0) = h(1 + \tanh(2x))/2$ and $u(x, 0) =$
 143 0 everywhere. A numerical simulation of equation (12) has been carried out
 144 with $g = 1$ and $h = 1$. The numerical and analytical surface profiles at $t = 0$
 145 and after the dam has broken are plotted in figure 1.

146 Within the framework of the KdV equation in the presence of vorticity, we
 147 have also checked that solitary waves are propagated with the right velocity
 148 that depends on Ω .

149 2.2 The boundary Integral Element Method

150 The problem considered here is identical to the one described in the previous
 151 section. It is two dimensional, and the current field is assumed to be steady,
 152 constant in the horizontal direction, and to vary linearly with depth,

$$U(z) = U_0 + \Omega z. \quad (14)$$

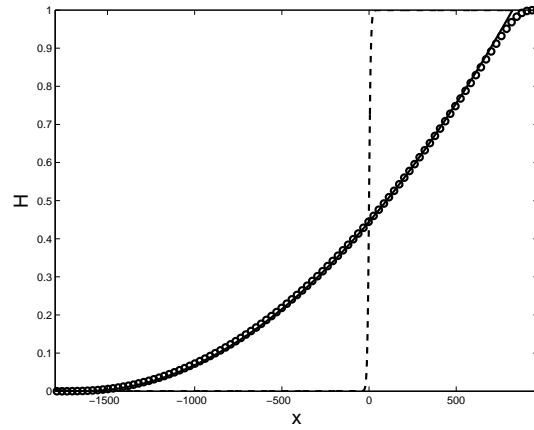


Fig. 1 Dam-break: comparison between analytical (solid line) and numerical solutions (o) after the dam has broken. The dashed line represents the initial condition at $t = 0$

153 The three dimensional interaction of water waves propagating obliquely in
 154 the assumed current are not considered here. The vorticity within the flow is
 155 thus constant, as previously mentioned. It is straightforward that such current,
 156 associated with hydrostatic pressure $P(z) = p_0 - gz$ is solution of the Euler
 157 equations when considering a problem of constant depth. This will allow to
 158 seek for wavy perturbations $(u(x, z, t), v(x, z, t))$ associated with the pressure
 159 field $p(x, z, t)$. The total flow fields are then given by

$$\begin{aligned}\tilde{u}(x, z, t) &= u(x, z, t) + U(z), \\ \tilde{v}(x, z, t) &= v(x, z, t) \quad \text{and} \\ \tilde{p}(x, z, t) &= p(x, z, t) + P(z).\end{aligned}\tag{15}$$

160 Using this decomposition, the Euler equations might reduce to

$$u_t + (U + u)u_x + vU_z + vu_z = -\frac{p_x}{\rho} \quad \text{and}\tag{16}$$

$$v_t + (U + u)v_x + vv_z + g = -\frac{p_z}{\rho},\tag{17}$$

161 which has to be fulfilled together with the continuity equation

$$u_x + v_z = 0.\tag{18}$$

162 As it is demonstrated in Simmen (1984), and more recently in Nwogu (2009),
 163 the wavy perturbations propagating in such current conditions are irrotational.
 164 Indeed, since the second derivative of the background current U_{zz} is nil, the
 165 vorticity conservation equation involves no source term, and the vorticity field
 166 does not exchange any vorticity with the wavy perturbations. Thus, we might
 167 introduce a velocity potential $\phi(x, z, t)$ from which derive the perturbation
 168 induced velocities ($\nabla\phi = (u, v)$). It has to be emphasized that the continuity
 169 equation (18) is automatically satisfied if the velocity potential is solution of
 170 Laplace's equation

$$\Delta\phi = 0. \quad (19)$$

171 The kinematic free surface condition might also be expressed, and if (X, Z)
 172 denotes the location of a particle at the free surface, this condition might be
 173 expressed

$$\frac{dX}{dt} = u \quad \text{and} \quad \frac{dZ}{dt} = v - U(\eta)\frac{\partial\eta}{\partial x}, \quad (20)$$

174 where d/dt refers to the material derivative $d/dt = \partial/\partial t + u\partial/\partial x + v\partial/\partial z$,
 175 and $Z = \eta(x, t)$.

176 Now, a stream function ψ can also be introduced, so that $(\partial\psi/\partial z, -\partial\psi/\partial x) =$
 177 (u, v) . The Euler equations (16) and (17) can now be integrated in space, and
 178 it comes

$$\frac{\partial\phi}{\partial t} + U(z)\frac{\partial\phi}{\partial x} + \frac{\nabla\phi^2}{2} - \Omega\psi + gz = -\frac{p}{\rho} \quad (21)$$

179 When applied to the free surface, where the pressure is constant, this equation
 180 provides the classical dynamic boundary condition. Introducing the material
 181 derivative used in the kinematic condition, this condition reduces to

$$\frac{d\phi}{dt} + U(\eta)\frac{\partial\phi}{\partial x} - \frac{\nabla\phi^2}{2} - \Omega\psi + g\eta = 0, \quad (22)$$

182 At this point, the knowledge of the stream function ψ at the free surface is
 183 still needed. Hopefully, one can notice the relationship

$$\frac{\partial\psi}{\partial\tau} = -\frac{\partial\phi}{\partial n}, \quad (23)$$

184 where $(\boldsymbol{\tau}, \mathbf{n})$ refer respectively to the tangential and normal vectors at the free
 185 surface. Thus, the stream function ψ can be evaluated at the free surface as

186 soon as the normal derivative of the velocity potential is known.

187 Furthermore, if equations (20), (22) and (23) refer to the boundary condition
188 at the free surface, the fluid domain still has to be closed. This is done by
189 using impermeability conditions on the bottom boundary condition, located
190 at $z = -h$, h being used as the reference length (i.e. $h = 1$) and on the vertical
191 boundary conditions, located respectively at $x = 0$ and $x = 200$.

192 The numerical approach used here has already been implemented and used
193 successfully in the framework of focusing wave groups in the presence of uni-
194 form current (Touboul et al (2007); Merkoune et al (2013)). The extension
195 allowing to take constant vorticity into account was presented in Touboul and
196 Kharif (2016) together with a validation of the approach. It is based on a
197 Boundary Integral Element Method (BIEM) coupled with a Mixed Euler La-
198 grange (MEL) procedure. At each time step, the Green's second identity is
199 discretized to solve numerically the Laplace equation (19). Thus, the potential
200 and its normal derivative are known numerically, and the stream function ψ
201 can be deduced by integration of equation (23) along the free surface. This
202 numerical integration is performed in the up-wave direction, starting from the
203 down-wave end of the basin, and using zero as initial value. Then, the time
204 stepping is performed by numerical integration of equations (20) and (22) us-
205 ing a fourth order Runge & Kutta scheme. Full details of the implementation
206 can be found in Touboul and Kharif (2010). In every simulations, the total
207 number of points considered at the free surface was $N_{fs} = 1000$, while the
208 total number of points used on the solid boundaries was $N_{bo} = 600$. The time
209 step used for the simulations was $dt = 0.01$.

210 2.3 Initial condition

211 Both numerical approaches described in previous subsections were initialised
212 with the same initial condition. Following the approach described in Kharif et al
213 (2000); Pelinovsky et al (2000), the initial condition is obtained numerically.
214 A Gaussian initial wave, with no initial velocity, is allowed to collapse under

215 gravity. This simulation is run in the absence of current and vorticity, using
216 the BIEM. Two radiated wave trains, propagating in opposite directions, are
217 generated. The wave group propagating in the $(-x)$ direction is isolated, and
218 space-time coordinates are reverted. This allows the generation of a focusing
219 wave group in shallow water conditions. For the numerical simulations con-
220 sidered here, the initial gaussian elevation has a maximum amplitude $a = h$
221 where h still being the reference length, and a width $\sigma = 2h$.

222 The wave train considered is used as initial condition for both numerical ap-
223 proaches. The surface elevation of this focusing wave group is used as initial
224 condition for the generalised-Whitham equation with vorticity, and for the
225 KdV equation with vorticity as well. Both elevations and velocity potential
226 are required to initialise the BIEM.

227 The dimensionless value of the maximum surface elevation of the wave group
228 obtained, $\eta_{\max}(t = 0)$, is 0.0715. The dynamics of this wave packet is illus-
229 trated in figure 2, in the framework of BIEM simulations. The initial wave
230 packet is propagated, and the effects of both nonlinearity and dispersion lead
231 to the formation of a high wave.

232 **3 Results and discussion**

233 Among the rogue wave properties, a particular attention is paid to the ampli-
234 fication factor of the maximum surface elevation, defined as $\eta_{\max}(t)/\eta_{\max}(t =$
235 $0)$. The time evolution of this amplification factor is plotted in figures 3-7 for
236 several values of the shear Ω . One can see that the evolutions computed with
237 the generalised Whitham equation and BIEM are similar even though the
238 amplification is overestimated with the generalised Whitham equation with
239 vorticity. The amplification factor at the focusing time t_f plotted in figure 8
240 increases as the shear Ω increases. One can observe that the difference between
241 the two curves decreases as the shear Ω increases. In other words, the agree-
242 ment is better for positive values of the shear Ω (negative vorticity) than for
243 negative values of Ω (positive vorticity). The KdV equation exhibits the same

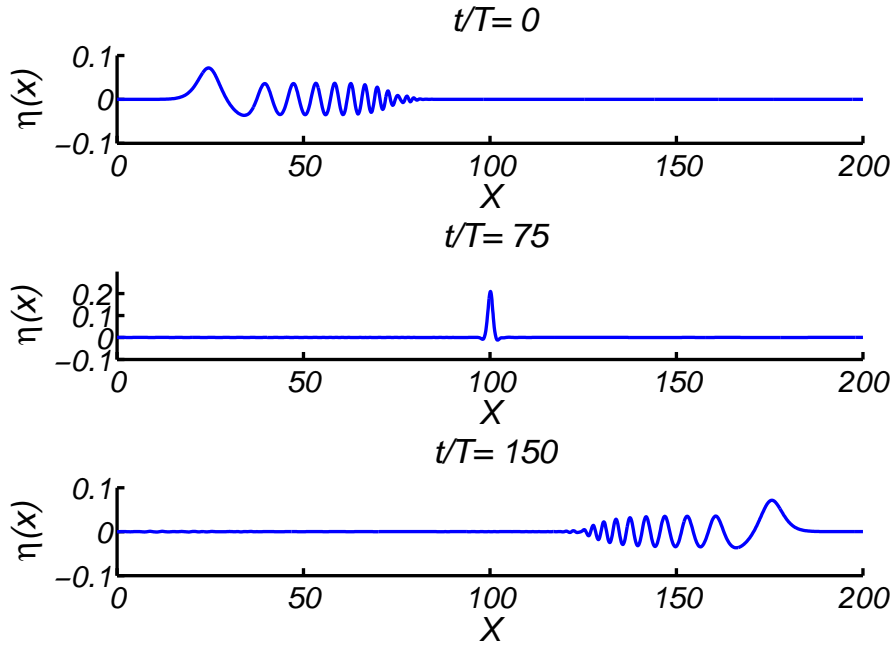


Fig. 2 Surface elevation of the focusing waves group evolving from initial condition ($t/T = 0$) to rogue wave occurrence ($t/T = 75$), before defocusing ($t/T = 150$).

244 tendency that is an increase of the maximum of amplification with Ω . The fo-
 245 cusing time t_f obtained with both models are very close. On the opposite, the
 246 KdV equation underestimates the maximum value of the amplification factor
 247 and the focusing time t_f as well. In figures 6 and 7, the BIEM shows for neg-
 248 ative values of the shear Ω first a reduction of the maximum surface elevation
 249 and then an amplification. This attenuation of the maximum of the surface
 250 elevation does not occur for the generalised Whitham and KdV equations. We
 251 define as extreme wave events or rogue waves those in the group whose surface
 252 elevation satisfies $\eta_{\max}(t = 0)/\eta_{\max}(t) \geq 2$. In that way, we can introduce the
 253 rogue wave lifetime which is the duration of the extreme wave event. In figure
 254 9 is shown this duration as a function of Ω . For positive values of the shear
 255 Ω the rogue wave duration is increased whereas it is the opposite for negative
 256 values.

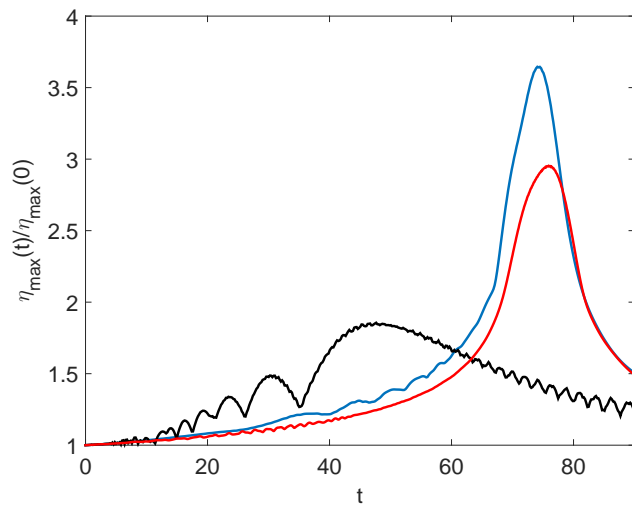


Fig. 3 (color online) Time evolution of the amplification factor without vorticity effect ($\Omega = 0$). Generalised Whitam equation (blue solid line), BIEM (red solid line) and KdV equation (black solid line)

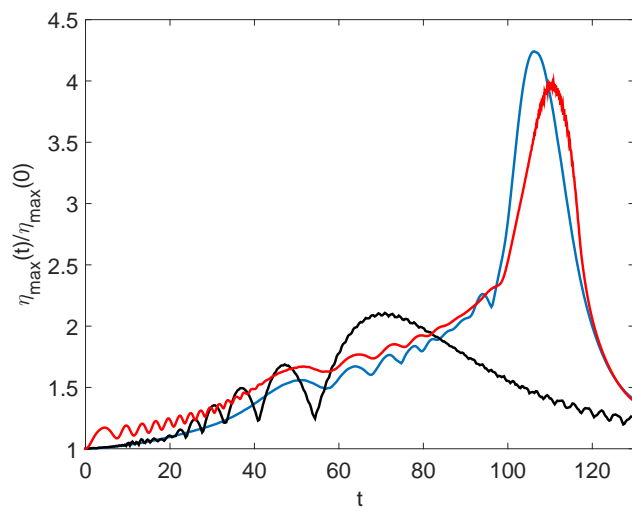


Fig. 4 (color online) Time evolution of the amplification factor with vorticity effect ($\Omega = 0.5$). Generalised Whitam equation (blue solid line), BIEM (red solid line) and KdV equation (black solid line)

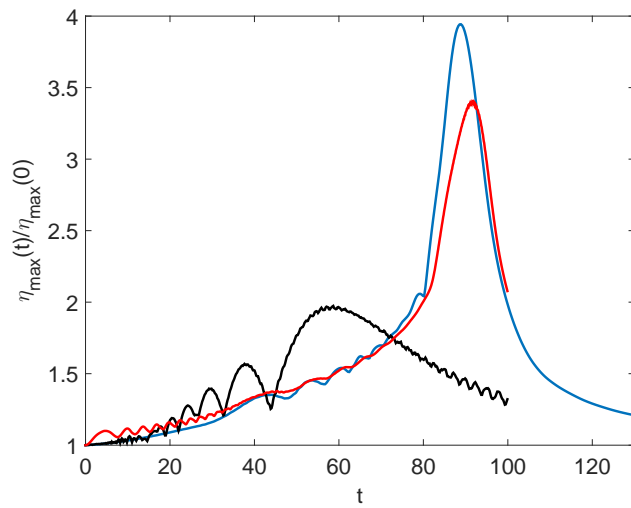


Fig. 5 (color online) Time evolution of the amplification factor with vorticity effect ($\Omega = 0.25$). Generalised Whitham equation (blue solid line), BIEM (red solid line) and KdV equation (black solid line)

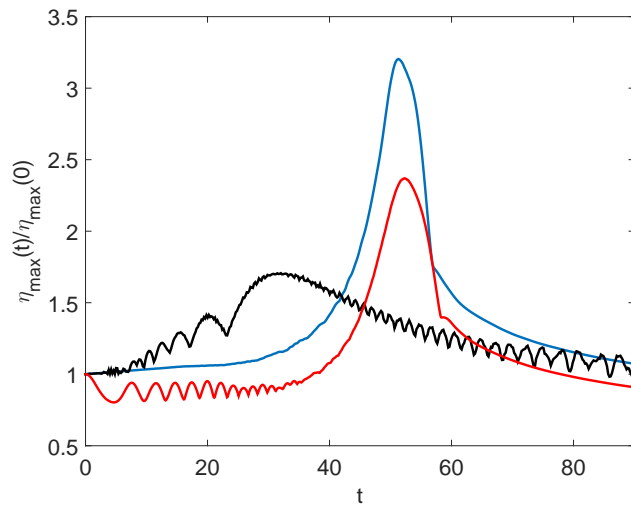


Fig. 6 (color online) Time evolution of the amplification factor with vorticity effect ($\Omega = -0.5$). Generalised Whitham equation (blue solid line), BIEM (red solid line) and KdV equation (black solid line)

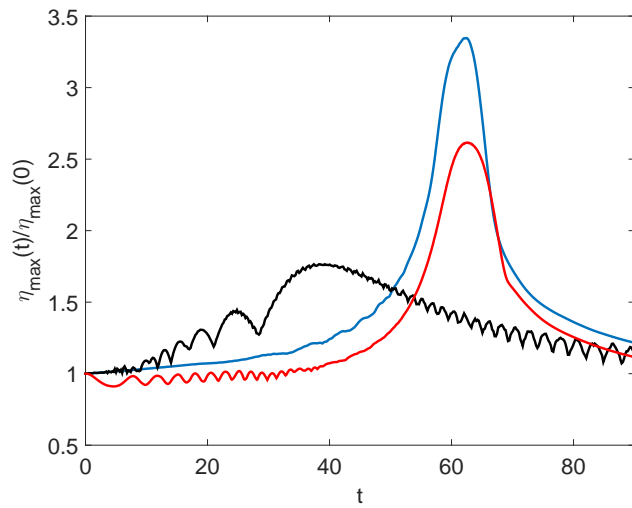


Fig. 7 (color online) Time evolution of the amplification factor with vorticity effect ($\Omega = -0.25$). Generalised Whitam equation (blue solid line), BIEM (red solid line) and KdV equation (black solid line)

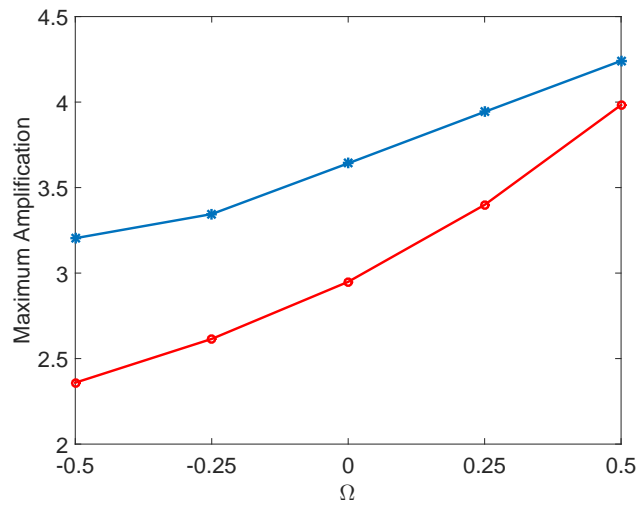


Fig. 8 (color online) Maximum amplification factor at the focusing time as a function of the shear intensity of the current. Generalised Whitam equation (blue solid line), BIEM (red solid line)

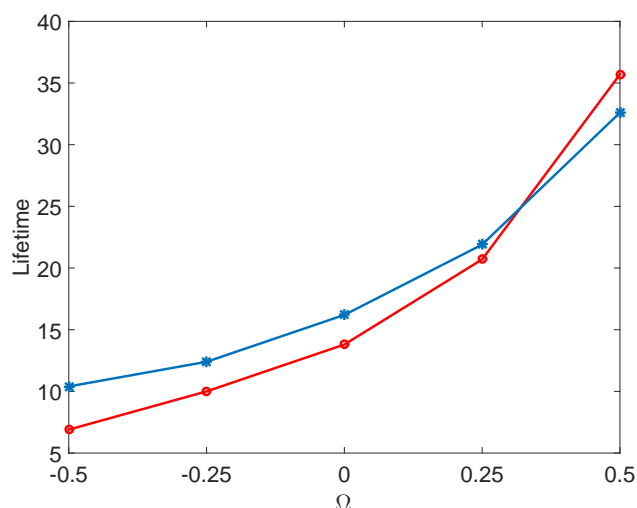


Fig. 9 (color online) Rogue wave duration as a function of the shear intensity of the current. Generalised Whitham equation (blue solid line), BIEM (red solid line)

258 4 Conclusion

259 The effect of an underlying vortical current on two-dimensional rogue wave
 260 properties has been investigated by using two different approaches in shallow
 261 water. One is based on a new approximate equation, the generalised Whitham
 262 equation with constant vorticity which is fully nonlinear and fully linear dis-
 263 persive whereas the other, the BIEM with constant vorticity, is fully nonlinear
 264 and fully nonlinear dispersive. Besides the study on vorticity effect on rogue
 265 waves, it is shown that the results of the generalised Whitham equation with
 266 vorticity are in agreement with those of the BIEM demonstrating that this
 267 new single nonlinear equation is an efficient model for the investigation of
 268 nonlinear long waves on vertically sheared current of constant vorticity.

269 The numerical simulations carried out with all the approaches have shown
 270 that the presence of vorticity modifies the rogue wave properties significantly.
 271 The maximum of amplification factor of the surface elevation increases as the
 272 shear intensity of the current increases. The lifetime of extreme wave event
 273 follows the same tendency.

274 **Acknowledgements** The authors would like to thank the French DGA, who supported
275 this work through the ANR grant ANR-13-ASTR-0007.

276 References

- 277 Chambarel J, Kharif C, Kimmoun O (2010) Generation of two-dimensional steep water
278 waves on finite depth with and without wind. *Eur J Mech B/Fluids* 29(2):132–142
- 279 Choi W (2003) Strongly nonlinear long gravity waves in uniform shear flows. *Phys Rev E*
280 68:026,305
- 281 Dysthe KI, Krogstad HE, Muller P (2008) Oceanic rogue waves. *Annu Rev Fluid Mech*
282 40:287–310
- 283 Freeman N, Johnson R (1970) Shallow water waves on shear flows. *J Fluid Mech* 42 (2):401–
284 409
- 285 Hur VM, Johnson MA (2015) Modulational instability in the whitham equation with surface
286 tension and vorticity. *Nonlinear Analysis* 129:104–118
- 287 Kharif C, Abid M (2017) Whitham approach for the study of nonlinear waves on a vertically
288 sheared current in shallow water. *J Fluid Mech* (in revision)
- 289 Kharif C, Pelinovsky E (2003) Physical mechanisms of the rogue wave phenomenon. *Eur J*
290 *Mech B/Fluids* 22:603–634
- 291 Kharif C, Pelinovsky E, Talipova T (2000) Formation de vagues géantes en eau peu profonde.
292 *CRAS* 328 (IIb):801–807
- 293 Kharif C, Pelynovsky E, Slunyaev A (2009) *Rogue waves in the ocean*. Springer
- 294 Merkoune D, Touboul J, Abcha N, Mouazé D, Ezersky A (2013) Focusing wave group on a
295 current of finite depth. *Nat Hazards Earth Syst Sci* 13:2941–2949
- 296 Nwogu OG (2009) Interaction of finite-amplitude waves with vertically sheared current fields.
297 *J Fluid Mech* 627:179–213
- 298 Onorato M, Residori S, Bertolozzo U, Montina A, Arecchi F (2013) Rogue waves and their
299 generating mechanisms in different physical contexts. *Phys Rep* 528:47–89
- 300 Pelinovsky E, Sergeeva A (2006) Numerical modeling of kdv random wave field. *Eur J Mech*
301 *B/Fluids* 25:425–434
- 302 Pelinovsky E, Talipova T, Kharif C (2000) Nonlinear dispersive mechanism of the freak wave
303 formation in shallow water. *Physica D* 147:83–94
- 304 Peterson P, Soomere T, Engelbrecht J, van Groesen E (2003) Interaction solitons as a
305 possible model for extreme waves in shallow water. *Nonlin Proc Geophys* 10:503–510
- 306 Simmen JA (1984) Steady deep-water waves on a linear shear current. PhD thesis, California
307 Institute of Technology, Pasadena, Californie
- 308 Simmen JA, Saffman PG (1985) Steady deep-water waves on a linear shear current. *Stud*
309 *Appl Math* 73:35–57

-
- 310 Soomere T, Engelbrecht (2005) Extreme evaluation and slopes of interacting solitons in
311 shallow water. *Wave Motion* 41:179–192
- 312 Talipova T, Kharif C, Giovanangeli J (2008) Modelling of rogue wave shapes in shallow
313 water. Springer, Eds. Pelinovsky E. and Kharif C.
- 314 Toffoli A, Onorato M, Osborne A, Monbaliu J (2006) Non-gaussian properties of surface
315 elevation in crossing sea states in shallow water. *Proc Int Conf Coast Eng (ICCE06 pp*
316 *782–790*
- 317 Touboul J, Kharif C (2010) Two-dimensional direct numerical simulations of the dynamics
318 of rogue waves under wind action, *Advances in numerical simulation of nonlinear water*
319 *waves*, vol 11, The world Scientific Publishing Co., London, chap 2
- 320 Touboul J, Kharif C (2016) Effect of vorticity on the generation of rogue waves due to
321 dispersive focusing. *Natural Hazards* 84(2):585–598
- 322 Touboul J, Pelinovsky E, Kharif C (2007) Nonlinear focusing wave groups on current. *Journ*
323 *Korean Soc Coast And Ocean Engineers* 19 (3):222–227
- 324 Whitham G (1974) *Linear and nonlinear waves*. John Wiley & Sons